

Hydrogen Bonding of β -Turn Structure Is Stabilized in D₂O

Yunhee Cho,[†] Laura B. Sagle,[†] Satoshi Iimura,[‡] Yanjie Zhang,[†] Jaibir Kherb,[†]
Ashutosh Chilkoti,[§] J. Martin Scholtz,[‡] and Paul S. Cremer^{*,†}

Department of Chemistry, Texas A&M University, 3255 TAMU, and Department of Molecular and Cellular Medicine, Texas A&M Health Science Center, College Station, Texas 77843, and Department of Biomedical Engineering, Duke University, Durham, North Carolina 27708

Received May 19, 2009; E-mail: cremer@mail.chem.tamu.edu

Abstract: The lower critical solution temperature (LCST) of elastin-like polypeptides (ELPs) was investigated as a function of ELP chain length and guest residue chemistry. These measurements were made in both D₂O and H₂O. Differences in the LCST values with heavy and light water were correlated with secondary structure formation of the polypeptide chains. Such structural information was obtained by circular dichroism and infrared measurements. Additional thermodynamic data were obtained by differential scanning calorimetry. It was found that there is a greater change in the LCST value between H₂O and D₂O for those polypeptides which form the greatest amount of β -turn/ β -aggregate structure. Moreover, these same molecules were the least hydrophobic ELPs. Therefore, hydrogen bonding rather than hydrophobicity was the key factor in the stabilization of the collapsed state of ELPs in D₂O compared with H₂O.

Introduction

Understanding protein stability and folding is of central importance in chemistry, biology, and medicine. Solvent isotope effects have provided important clues about the stability of various structural units found in folded proteins. Specifically, previous studies comparing protein stability in D₂O vs H₂O have shown that the folded state is often, but not always, stabilized in D₂O.^{1–5} For example, proteins possessing mostly β -type structures are preferentially stabilized in D₂O, while α -helical structures show the opposite trend.^{6–8} These observations are usually attributed to one of two effects: (1) D₂O may modulate hydrophobic interactions in proteins or (2) D₂O may selectively stabilize/destabilize inter- and/or intramolecular hydrogen bonds that are more prevalent in the folded state of proteins.^{9–17}

To access the relative influences of hydrogen bonding and hydrophobic interactions on β -structure formation, one must be

able to parse their contributions separately. Unfortunately, due to the inherent complexity of proteins, systematically altering global hydrophobicity through mutagenesis without changing protein structure is an extraordinarily difficult task.¹⁸ This task can be made easier, however, by employing a biopolymer rather than a fully structured protein. With this rationale in mind, we have chosen to investigate elastin-like polypeptides (ELPs) to elucidate the relative contribution of hydrogen bonding and hydrophobic interactions to β -structure formation. ELPs consist of the pentapeptide repeat unit Val-Pro-Gly-Xaa-Gly, where Xaa can be any residue except proline. ELPs are highly soluble in aqueous solution, but upon raising the temperature, they undergo hydrophobic collapse accompanied by an increase in secondary/tertiary structure formation much like folded proteins.^{19–25} The temperature at which this transition occurs is referred to as the lower critical solution temperature (LCST).^{26–32}

[†] Texas A&M University.

[‡] Texas A&M Health Science Center.

[§] Duke University.

- (1) Antonino, L. C.; Kautz, R. A.; Nakano, T.; Fox, R. O.; Fink, A. L. *Proc. Natl. Acad. Sci. U.S.A.* **1991**, *88*, 7715–7718.
- (2) Guzzi, R.; Sportelli, L.; La Rosa, C.; Milardi, D.; Grasso, D. *J. Phys. Chem. B* **1998**, *102*, 1021–1028.
- (3) Huyghues-Despointes, B. M. P.; Scholtz, J. M.; Pace, C. N. *Nat. Struct. Biol.* **1999**, *6*, 910–912.
- (4) Kuhlman, B.; Raleigh, D. P. *Protein Sci.* **1998**, *7*, 2405–2412.
- (5) Makhatadze, G. I.; Clore, G. M.; Gronenborn, A. M. *Nat. Struct. Biol.* **1995**, *2*, 852–855.
- (6) Bowers, P. M.; Klevit, R. E. *Nat. Struct. Biol.* **1996**, *3*, 522–531.
- (7) Parker, M. J.; Clarke, A. R. *Biochemistry* **1997**, *36*, 5786–5794.
- (8) Shi, Z. S.; Krantz, B. A.; Kallenbach, N.; Sosnick, T. R. *Biochemistry* **2002**, *41*, 2120–2129.
- (9) Baghurst, P. A.; Sawyer, W. H.; Nichol, L. W. *J. Biol. Chem.* **1972**, *247*, 3198–3204.
- (10) Efimova, Y. M.; Haemers, S.; Wierczinski, B.; Norde, W.; van Well, A. A. *Biopolymers* **2007**, *85*, 264–273.
- (11) Gomezpuyou, M. T. D.; Gomezpuyou, A.; Cerbon, J. *Arch. Biochem. Biophys.* **1978**, *187*, 72–77.
- (12) Guzzi, R.; Arcangeli, C.; Bizzarri, A. R. *Biophys. Chem.* **1999**, *82*, 9–22.

- (13) Hattori, A.; Crespi, H. L.; Katz, J. J. *Biochemistry* **1965**, *4*, 1213–1225.
- (14) Henderson, R. F.; Henderson, T. R.; Woodfin, B. M. *J. Biol. Chem.* **1970**, *245*, 3733–3737.
- (15) Kresheck, G. C.; Schneider, H.; Scheraga, H. A. *J. Phys. Chem.* **1965**, *69*, 3132–3144.
- (16) Masson, P.; Laurentie, M. *Biochim. Biophys. Acta* **1988**, *957*, 111–121.
- (17) Sheu, S. Y.; Schlag, E. W.; Selzle, H. L.; Yang, D. Y. *J. Phys. Chem. A* **2008**, *112*, 797–802.
- (18) Sulistijo, E. S.; MacKenzie, K. R. *J. Mol. Biol.* **2006**, *364*, 974–990.
- (19) Flamia, R.; Zhdan, P. A.; Martino, M.; Castle, J. E.; Tamburro, A. M. *Biomacromolecules* **2004**, *5*, 1511–1518.
- (20) Kumashiro, K. K.; Kurano, T. L.; Niemczura, W. P.; Martino, M.; Tamburro, A. M. *Biopolymers* **2003**, *70*, 221–226.
- (21) Ohgo, K.; Ashida, J.; Kumashiro, K. K.; Asakura, T. *Macromolecules* **2005**, *38*, 6038–6047.
- (22) Ohgo, K.; Kurano, T. L.; Kumashiro, K. K.; Asakura, T. *Biomacromolecules* **2004**, *5*, 744–750.
- (23) Schmidt, P.; Dybal, J.; Rodriguez-Cabello, J. C.; Rebotto, V. *Biomacromolecules* **2005**, *6*, 697–706.
- (24) Urry, D. W. *J. Phys. Chem. B* **1997**, *101*, 11007–11028.
- (25) Yao, X. L.; Hong, M. *J. Am. Chem. Soc.* **2004**, *126*, 4199–4210.

The hydrophobicity of ELPs can be systematically tuned by simply replacing the guest residues with more or less hydrophobic amino acids or by changing the chain length of an otherwise identical sequence.^{33,34} As such, we have compared the LCST of ELPs of different amino acid compositions and chain lengths in H₂O and D₂O. The five ELPs employed in this study were V₅-120, QV₆-112, V₅A₂G₃-330, V₅A₂G₃-120, and V₅A₂G₃-60. ELP V₅-120 contains valine residues in all the guest sites and therefore consists of 120 repeats of VPGVG for a total of 600 residues. By contrast, ELP V₅A₂G₃-60 contains 300 total residues whereby valine, alanine, and glycine are present in the X position in a 5:2:3 ratio. ELP QV₆-112 contains 560 residues in which glutamine and valine are present in a 1:6 ratio.

Although the structure of the collapsed state of ELPs has not been completely determined, it is believed to involve type II β -turn formation which consists of hydrogen bonds formed between the first and fourth residues in the pentapeptide repeats.^{24,25,35} Some reports have suggested that β -spiral, β -aggregate, or distorted β -sheet structures may also be present under some conditions.^{34,36–40} More significantly, as we will show, all five of the ELPs studied herein possess the same structural motifs in both the collapsed and uncollapsed states. The relative amounts of these structural motifs, however, change as a function of the hydrophobicity of the individual ELPs. These changes provide key evidence about the stabilization mechanism of ELPs in D₂O.

Herein, the mechanism for the stabilization of the hydrophobic collapse of five ELPs in D₂O was investigated by four complementary techniques. Phase transition measurements revealed an inverse correlation between the change in the LCST value and the hydrophobicity of the ELPs. Since increasing hydrophobicity did not increase the collapsed state's stability in D₂O, it was hypothesized that hydrogen bonding and structure formation would instead be the dominant factors. Therefore, secondary structure determination of the five ELPs was carried out using circular dichroism (CD) spectroscopy just below the phase transition temperature. It was found that there is less random coil and more β -turn structure in shorter chain length macromolecules as well as those that contained fewer hydrophobic residues. Moreover, amide I band Fourier transform infrared (FTIR) spectroscopy measurements showed the trends observed in CD spectroscopy carried over to the collapsed state of the polypeptides. In fact, a direct correlation between the

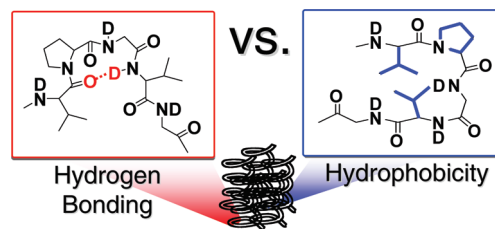


Figure 1. Schematic diagram of a portion of an ELP highlighting (a) hydrogen bond formation in the β -turn structure vs (b) the presence of hydrophobic residues.

amount of β -turn structure found by FTIR measurements and the difference in the LCST between D₂O and H₂O (the Δ LCST value) was observed. Finally, differential scanning calorimetry (DSC) was used to probe the relationship between enthalpic changes upon hydrophobic collapse and secondary structure formation. Again, a strong direct correlation was observed. These results suggested that hydrogen bonding related to structure formation rather than hydrophobicity was the key factor in the stabilization of the folded state of ELPs in D₂O vs H₂O (Figure 1).

Materials and Methods

ELP Preparation and LCST Measurements. The pET plasmids of five ELPs were constructed by the recursive directional ligation method.³³ The plasmids were expressed in BLR/DE3 *Escherichia coli* in TB dry medium with the addition of ampicillin.²⁶ The cells were expressed for 24 h at 37 °C and then lysed by sonication. Purification of the ELPs was accomplished via inverse phase transition cycling. After three cycles, the samples were dialyzed against purified water (NANOpure Ultrapure Water System, Barnstead, Dubuque, IA) with a minimum resistivity of 18 M Ω ·cm to remove residual salts. A sodium dodecyl sulfate–polyacrylamide gel was used to verify the purity of the final ELP product. The polypeptide concentration was determined by UV absorbance measurements with an extinction coefficient of 5690 M⁻¹ cm⁻¹ at 280 nm. The samples were lyophilized and stored at –80 °C until use.

Purified water was employed for all thermodynamic and spectroscopic experiments performed in H₂O. On the other hand, D₂O from Cambridge Isotope Laboratories, Inc. (>99.9% purity) was used for all analogous experiments in heavy water, and these solutions were not further purified. ELP solutions were prepared in their respective solvents without additional salt at a polypeptide concentration of 6.4 mg/mL. The LCST values of the ELP solutions were measured with a temperature gradient microfluidic platform placed under a dark field microscope as previously described.^{41–45}

Circular Dichroism. CD measurements were taken with an AVIV 62DS spectropolarimeter using a NesLab Coolflow CFT-33 refrigerated circulator. The conversion of the CD signal, which is the difference in absorption minus the background, Δm° , to mean residue ellipticity, $[\theta]_{\text{obsd}}$ was done using the following equation:

$$[\theta]_{\text{obsd}} = \frac{100\Delta m^\circ}{Cnl} \quad (1)$$

- (26) Cho, Y.; Zhang, Y. J.; Christensen, T.; Sagle, L. B.; Chilkoti, A.; Cremer, P. S. *J. Phys. Chem. B* **2008**, *112*, 13765–13771.
 (27) Meyer, D. E.; Chilkoti, A. *Nat. Biotechnol.* **1999**, *17*, 1112–1115.
 (28) Meyer, D. E.; Trabbic-Carlson, K.; Chilkoti, A. *Biotechnol. Prog.* **2001**, *17*, 720–728.
 (29) Nath, N.; Chilkoti, A. *J. Am. Chem. Soc.* **2001**, *123*, 8197–8202.
 (30) Reguera, J.; Urry, D. W.; Parker, T. M.; McPherson, D. T.; Rodriguez-Cabello, J. C. *Biomacromolecules* **2007**, *8*, 354–358.
 (31) Trabbic-Carlson, K.; Meyer, D. E.; Liu, L.; Piervincenzi, R.; Nath, N.; LaBean, T.; Chilkoti, A. *Protein Eng. Des. Sel.* **2004**, *17*, 57–66.
 (32) Urry, D. W.; Luan, C. H.; Parker, T. M.; Gowda, D. C.; Prasad, K. U.; Reid, M. C.; Safavy, A. *J. Am. Chem. Soc.* **1991**, *113*, 4346–4348.
 (33) Meyer, D. E.; Chilkoti, A. *Biomacromolecules* **2002**, *3*, 357–367.
 (34) Nuhn, H.; Klok, H. A. *Biomacromolecules* **2008**, *9*, 2755–2763.
 (35) Urry, D. W.; Long, M. M. *Crit. Rev. Biochem.* **1976**, *4*, 1–45.
 (36) Venkatachalam, C. M.; Urry, D. W. *Macromolecules* **1981**, *14*, 1225–1229.
 (37) Gross, P. C.; Possart, W.; Zeppezauer, M. *Z. Naturforsch., C* **2003**, *58*, 873–878.
 (38) Martino, M.; Bavoso, A.; Guantieri, V.; Coviello, A.; Tamburro, A. M. *J. Mol. Struct.* **2000**, *519*, 173–189.
 (39) Ostuni, A.; Bochicchio, B.; Armentano, M. F.; Bisaccia, F.; Tamburro, A. M. *Biophys. J.* **2007**, *93*, 3640–3651.
 (40) Tamburro, A. M.; Bochicchio, B.; Pepe, A. *Biochemistry* **2003**, *42*, 13347–13362.

- (41) Mao, H. B.; Holden, M. A.; You, M.; Cremer, P. S. *Anal. Chem.* **2002**, *74*, 5071–5075.
 (42) Mao, H. B.; Li, C. M.; Zhang, Y. J.; Bergbreiter, D. E.; Cremer, P. S. *J. Am. Chem. Soc.* **2003**, *125*, 2850–2851.
 (43) Mao, H. B.; Yang, T. L.; Cremer, P. S. *J. Am. Chem. Soc.* **2002**, *124*, 4432–4435.
 (44) Zhang, Y. J.; Furyk, S.; Sagle, L. B.; Cho, Y.; Bergbreiter, D. E.; Cremer, P. S. *J. Phys. Chem. C* **2007**, *111*, 8916–8924.
 (45) Zhang, Y. J.; Mao, H. B.; Cremer, P. S. *J. Am. Chem. Soc.* **2003**, *125*, 15630–15635.

Table 1. LCST Values ($^{\circ}\text{C}$) of Five ELPs in H_2O and D_2O at 6.4 mg/mL

	V ₅ -120	QV ₆ -112	V ₅ A ₂ G ₃ -330	V ₅ A ₂ G ₃ -120	V ₅ A ₂ G ₃ -60
H_2O	28.5 \pm 0.2	33.1 \pm 0.2	40.6 \pm 0.3	46.1 \pm 0.2	50.7 \pm 0.2
D_2O	26.5 \pm 0.2	30.4 \pm 0.3	36.6 \pm 0.2	40.9 \pm 0.2	45.1 \pm 0.2
ΔLCST	2.0 \pm 0.3	2.7 \pm 0.4	4.0 \pm 0.4	5.1 \pm 0.3	5.6 \pm 0.3

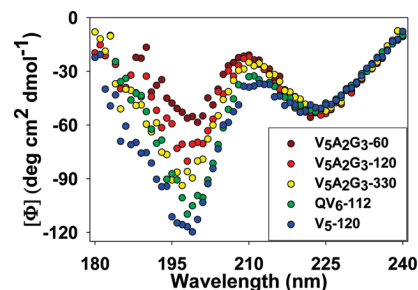
where C is the polypeptide concentration (mM), n is the number of residues in the polypeptide, and l is the path length (cm).⁴⁶ It should be noted that $[\theta]_{\text{obsd}}$ has units of $(\text{deg} \cdot \text{cm}^2)/\text{dmol}$. CD spectra were taken every 1 nm between 185 and 240 nm with 20 s averaging times. Samples were degassed prior to each measurement and placed in a cuvette with a 1 mm path length. Random coil and β -turn structures were confirmed by monitoring the ellipticity near 198 and 210 nm, respectively, in both D_2O , and H_2O solutions.

Amide I Band ATR/FTIR Measurements. Infrared spectra were taken with a Nicolet 470 FTIR spectrometer equipped with a liquid nitrogen cooled MCT detector (Thermo Electron Corp., Madison, WI) and a Pike Miracle attenuated total reflection (ATR) setup with a ZnSe (single bounce) crystal (Pike Technologies, Madison WI). The temperature of the sample stage was controlled with a circulation bath for measurements above the phase transition temperature of the ELP samples. To initiate data collection, a 20 μL ELP solution was placed in a Teflon well on top of the ZnSe crystal, and the cloudiness of the sample solution was monitored to ensure the phase transition had occurred. Spectra were constructed from 256 scans at 2 cm^{-1} resolution over a range from 4000 to 400 cm^{-1} . Background spectra were taken immediately before the samples were probed and subtracted automatically from the sample data. For each ELP sample, a corresponding spectrum from a pure D_2O solution was also obtained and then subtracted from the first spectrum. Baseline correction was carried out in Matlab (Mathworks, Natick, MA) by subtracting polynomials to flatten the baseline around the amide peaks. Spectral fitting was also carried out in Matlab with frequencies restricted to a 10 cm^{-1} window, but with unrestricted line widths. The spectral fits were obtained by minimization of the least error sum.

DSC Measurements. Differential scanning calorimetry measurements were made with a VP-DSC microcalorimeter (Microcal, LLC) at a temperature ramping rate of 0.5 $^{\circ}\text{C}/\text{min}$. All five ELPs were measured in D_2O and H_2O . These solutions were passed through a 0.2 μm pore size syringe filter followed by degassing for 10 min prior to use. Pure H_2O and D_2O were used as reference solutions. Aliquots of 500 μL of degassed sample and reference solutions were loaded into the sample holder with a syringe. Samples were cooled to 15 $^{\circ}\text{C}$ and held there for 30 min before the beginning of each scan. Data points were taken up to 15 $^{\circ}\text{C}$ above the phase transition temperature of the respective samples. Baseline correction was done in Origin 7J (OriginLab, Northampton, MA). Curve fitting was carried out in Origin 7J with an exponentially modified Gaussian function. The quality of the fits was judged by the least error sum method.

Results

LCST Values for ELPs in H_2O and D_2O . In a first set of experiments, the phase transition temperatures of all five ELPs were measured in both H_2O and D_2O with 6.4 mg/mL polypeptide by temperature gradient microfluidics. These LCST values are reported in Table 1. The LCST value in H_2O minus the LCST value in D_2O is listed as ΔLCST in the last row. As can be seen, the LCST was lower in D_2O under all circumstances, which indicates that this solvent better stabilized the hydrophobically collapsed state compared with H_2O . Intriguingly, however, the magnitude of ΔLCST showed an inverse

**Figure 2.** CD spectra of the five ELP solutions at a concentration of 0.32 mg/mL.

correlation with the hydrophobicity of the polypeptide. Thus, the ELPs which were most stabilized in D_2O possessed fewer hydrophobic amino acids or a shorter chain length in the case of the three polypeptides of constant chemical composition. These measurements strongly indicated that hydrophobicity was not the driving force for the relative stabilization of the collapsed state of the ELPs in D_2O .

It should be noted that the LCST of poly(*N*-isopropylacrylamide) (PNIPAM), another thermoresponsive polymer, is higher in D_2O than that in H_2O .⁴⁷ As PNIPAM undergoes entropically driven hydrophobic collapse in a manner similar to that of ELPs,⁴⁸ it is at least feasible that this difference arises primarily due to the lack of structure in PNIPAM molecules relative to ELPs. While ELPs and most structured proteins contain approximately 60% intra- and/or intermolecular hydrogen bonds in the collapsed state,^{49,50} PNIPAM only contains $\sim 10\%$ hydrogen bonds.⁵¹ Therefore, we performed circular dichroism and infrared spectroscopy measurements to probe the differences in the amount of structure formed for each of the five ELPs to determine whether there was a trend.

Secondary Structure of ELPs Probed by CD. Circular dichroism was employed to determine whether less hydrophobic and shorter ELPs (i.e., V₅A₂G₃-60) possessed greater amounts of secondary structure relative to more hydrophobic macromolecules (i.e., V₅-120) just below their respective phase transition temperatures. Specifically, all five ELPs were compared in H_2O 5 $^{\circ}\text{C}$ below their individual LCST values, and the data are shown in Figure 2. As can be seen, all five spectra showed clear evidence for two main features, a negative band at ~ 198 nm and a positive band at ~ 212 nm. According to accepted literature assignments,^{34,52–54} the former is most likely due to a random coil conformation, while the latter should arise from a type II β -turn structure. An alternative assignment of both peaks to polyproline II structure is also technically possible.^{38–40,55} This assignment could be ruled out by raising the temperature of the solution, which causes the 198 nm band to decrease and the 212 nm band to increase (see the Supporting Information).

(47) Kujawa, P.; Winnik, F. M. *Macromolecules* **2001**, *34*, 4130–4135.(48) Laukkanen, A.; Valtola, L.; Winnik, F. M.; Tenhu, H. *Macromolecules* **2004**, *37*, 2268–2274.(49) Baker, E. N.; Hubbard, R. E. *Prog. Biophys. Mol. Biol.* **1984**, *44*, 97–179.(50) Debelle, L.; Alix, A. J. P.; Jacob, M. P.; Huvenne, J. P.; Berjot, M.; Sombret, B.; Legrand, P. *J. Biol. Chem.* **1995**, *270*, 26099–26103.(51) Maeda, Y.; Higuchi, T.; Ikeda, I. *Langmuir* **2000**, *16*, 7503–7509.(52) Reiersen, H.; Clarke, A. R.; Rees, A. R. *J. Mol. Biol.* **1998**, *283*, 255–264.(53) Yamaoka, T.; Tamura, T.; Seto, Y.; Tada, T.; Kunugi, S.; Tirrell, D. A. *Biomacromolecules* **2003**, *4*, 1680–1685.(54) Nicolini, C.; Ravindra, R.; Ludolph, B.; Winter, R. *Biophys. J.* **2004**, *86*, 1385–1392.(55) Tamburro, A. M. *Nanomedicine* **2009**, *4*, 469–487.(46) Myers, J. K.; Pace, C. N.; Scholtz, J. M. *Protein Sci.* **1998**, *7*, 383–388.

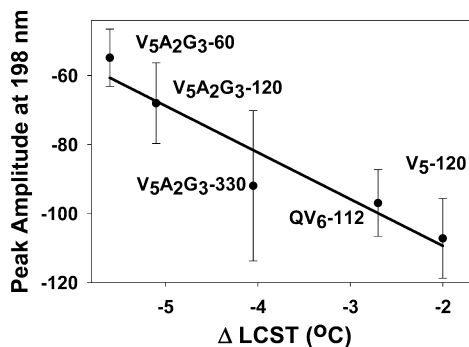


Figure 3. Peak amplitude at 198 nm vs Δ LCST for the five ELPs.

Therefore, the two bands were almost certainly not from the same structural component.^{38,39} Moreover, increasing the temperature of an ELP solution near the LCST should induce more β -turn structure formation^{34,36,53,54,56,57} while reducing random coil formation, which is consistent with our measurements. Finally, it can be clearly seen that the more hydrophobic ELPs showed less structure. This was evidenced by the greater dip near 198 nm as well as the smaller peak near 212 nm for these ELPs. The ordering of the peaks followed the same ordering of the Δ LCST values in Table 1. Moreover, the amplitude of the 198 nm peak showed a linear relationship to the Δ LCST values (Figure 3). This means that those ELPs which contained more random coil structure showed a smaller difference in stability in H₂O vs D₂O.

ATR/FTIR Measurements of the Collapsed State of ELPs. Amide I band ATR/FTIR studies were performed to investigate structural differences in ELPs of increasing hydrophobicity in the collapsed state. Unlike CD, FTIR spectroscopy is particularly useful for probing the collapsed state of the biopolymers since light scattering is not nearly as problematic at IR wavelengths. FTIR spectra were collected from all five ELPs above their LCSTs (70 °C) with a 6.4 mg/mL concentration of the polypeptides. The amide I band region in the IR spectra from the five ELPs is shown in Figure 4. The spectra fit extremely well to three Gaussian peaks. These resonances were centered near 1619, 1644, and 1663 cm⁻¹. As can be seen from the fitting, the highest and lowest frequency data (fit with blue curves) moved in concert. When their combined intensity was high, the central peak (fit with a green curve) was correspondingly low and vice versa.

Several laboratories have assigned the amide I peaks for ELPs.^{37,54,58} On the basis of these references, the peaks near 1619 and 1663 cm⁻¹ most likely arise from β -turn and β -aggregate structure. On the other hand, the resonance near 1644 cm⁻¹ can be assigned to random coil and perhaps some distorted β -sheet structure. Therefore, it appears that the satellite peaks represent better ordering in the collapsed state, while greater intensity in the central peak is associated with less secondary structure. This notion is consistent with the CD data, in which the most hydrophobic polypeptides showed the most random coil structure. Indeed, the amount of random coil structure preserved upon collapse should probably reflect the amount that was initially present in the uncollapsed state for these intrinsically disordered macromolecules.

Significantly, all five ELPs gave rise to identical spectroscopic features in both the CD and infrared spectra. Therefore, it appears

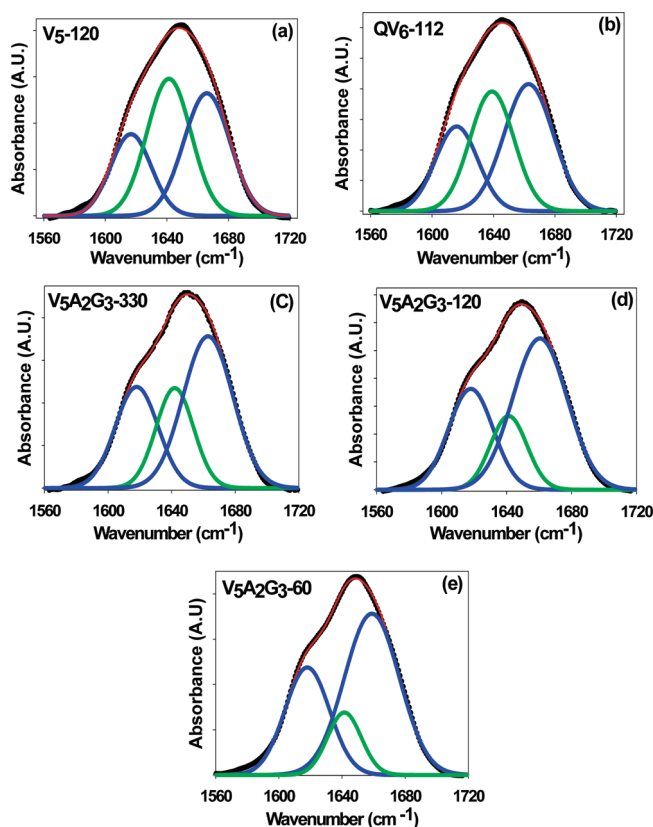


Figure 4. Fitted FTIR spectra (the red line represents the overall fit to three Gaussian peaks) of the collapsed state of the five ELPs: (a) V₅-120, (b) QV₆-112, (c) V₅A₂G₃-330, (d) V₅A₂G₃-120, and (e) V₅A₂G₃-60.

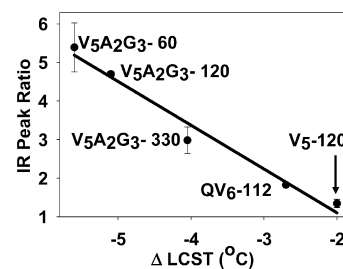


Figure 5. IR peak area ratio of (1619 + 1663 cm⁻¹)/1644 cm⁻¹ vs Δ LCST for the five ELPs.

that altering the identity of the guest residues and the chain length of the macromolecules had only limited influence on the types of structural motifs found for these five ELPs. The relative ratios for these two types of structures, however, do vary significantly with the hydrophobicity of the biomacromolecules. This idea can be quantified by calculating the sum of the area under the 1619 and 1663 cm⁻¹ peaks and dividing it by the area under the 1644 cm⁻¹ peak. This ratio is plotted against Δ LCST for all five ELPs in Figure 5. Strikingly, there is a direct correlation between the difference in the LCST value of a given ELP in H₂O vs D₂O and the value of the infrared data ratio. Therefore, the relative quantity of β -turn/ β -aggregate structure can be directly linked to the stabilization of the collapsed state of a given ELP in D₂O.

Calorimetry Measurements for ELP Collapse in H₂O and D₂O. In the final set of experiments, differential scanning calorimetry measurements were carried out with all five ELPs

(56) Urry, D. W. *J. Protein Chem.* **1984**, *3*, 403–436.

(57) Urry, D. W. *Angew. Chem., Int. Ed.* **1993**, *32*, 819–841.

(58) Serrano, V.; Liu, W.; Franzen, S. *Biophys. J.* **2007**, *93*, 2429–2435.

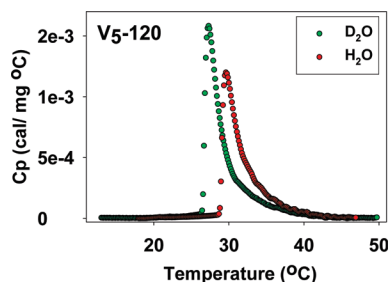


Figure 6. DSC scans of 6.4 mg/mL ELP V₅-120 solution in D₂O (green) and in H₂O (red).

Table 2. ΔH and $\Delta\Delta H$ Values for the Five ELPs in H₂O and D₂O

	ΔH_{H_2O} (cal/g)	ΔH_{D_2O} (cal/g)	$\Delta\Delta H_{DH}$ (cal/g)
V ₅ -120	4.39 ± 0.03	5.17 ± 0.03	0.78 ± 0.04
QV ₆ -112	3.11 ± 0.06	3.79 ± 0.07	0.68 ± 0.09
V ₅ A ₂ G ₃ -330	1.06 ± 0.11	1.45 ± 0.10	0.39 ± 0.15
V ₅ A ₂ G ₃ -120	1.43 ± 0.04	1.77 ± 0.05	0.34 ± 0.06
V ₅ A ₂ G ₃ -60	0.96 ± 0.06	1.18 ± 0.05	0.22 ± 0.08
PNIPAM	7.59	10.97	3.38

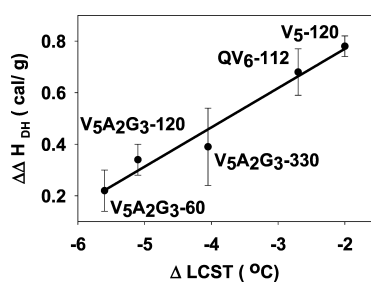


Figure 7. Correlation plot of $\Delta\Delta H$ vs $\Delta LCST$ for the five ELPs.

in D₂O and H₂O. Sample DSC data for V₅-120 are shown in Figure 6, and the data for the other four ELPs are provided in the Supporting Information. As can be seen, the thermograms have an asymmetric line shape. This arises because the LCST is followed immediately by the formation of a coacervate, which is denoted as an aqueous two-phase system (ATPS).^{45,59} The areas under the curves represent the change in enthalpy for the entire phase transition process (LCST + ATPS). The thermodynamic values for the total enthalpic change upon hydrophobic collapse and ATPS formation are listed in Table 2. Additionally, the value for PNIPAM is also provided as a comparison, although this macromolecule does not undergo ATPS formation. As can be seen, the phase transition for the ELPs and PNIPAM was endothermic in all cases in both solvents. Moreover, the change in enthalpy was always greater in D₂O. This unfavorable enthalpic change upon going from H₂O to D₂O was smallest for the shortest and least hydrophobic ELPs and directly correlated with the $\Delta LCST$ value for all five ELPs (Figure 7). Therefore, the differences in enthalpy gain can also be directly correlated with β -turn/ β -aggregate formation determined by FTIR (Figures 4 and 5). This means that the thermodynamics of the phase transition are directly correlated with the spectroscopic data.

Discussion

Two of the most widely studied systems which display lower critical solution temperature behavior are ELPs and

PNIPAM. The driving force for the phase transition of these systems is generally believed to involve the liberation of bound water molecules into the surrounding solution. As such, the free energy of the transition is expected to be negative in both cases on entropic grounds.^{51,60,61} Nevertheless, there should be a critical difference between these systems. As shown in Table 2 and Figure 7, the enthalpic cost of undergoing the hydrophobic collapse for ELPs increased as the hydrophobicity increased. Moreover, $\Delta\Delta H_{DH}$ was largest for the most hydrophobic ELPs. Therefore, the free energy gain was smallest for the most hydrophobic molecules. This manifested itself as smaller $\Delta LCST$ values for the most hydrophobic polypeptides.

As noted above and in contrast with ELPs, $\Delta LCST$ is actually negative for PNIPAM. Specifically, the phase transition temperature is about 1 °C higher for PNIPAM in D₂O than in H₂O.⁴⁷ Moreover, the enthalpic cost for undergoing the inverse phase transition in D₂O vs H₂O is very large in PNIPAM compared with ELPs (Table 2). This fact is particularly noteworthy as PNIPAM remains unstructured with minimal additional hydrogen bonding upon hydrophobic collapse.^{47,48,51,62} Moreover, one might have otherwise expected PNIPAM to have had a smaller overall enthalpic change for its phase transition than ELPs as there is no ATPS to make contributions in addition to the LCST. These facts provide important corroborating evidence for the hypothesis that it is the more extensive hydrogen bonding found in the least hydrophobic ELPs which is directly responsible for their smaller enthalpic cost of undergoing the phase transition. As such, β -turn/ β -aggregate formation can be correlated with the lowering of the LCST in D₂O and, hence, the stability of the collapsed state in heavy water (Figures 2–5).

The methods employed herein for understanding the relative importance of hydrogen bond formation vs hydrophobicity in stabilizing the collapsed structure of ELPs should be quite general. In the present case, the systems that were investigated contained mostly uncharged and nonpolar side chains. In fact, the only charged residues in these biomacromolecules came from the ends of the polymer chains and accounted for no more than 1% of the residues in all cases.⁶³ Even QV₆-112 contained only 1 polar residue for every 35-residue sequence. On the other hand, most structured proteins contain numerous positively charged, negatively charged, and polar residues. ELPs could be employed to address questions concerning the role that D₂O plays in stabilizing or destabilizing structure formation in those cases. For example, ELP constructs containing D, E, K, or R guest residues could be tested to probe the individual roles that specific charges play in stabilizing or destabilizing proteins in heavy water. Alternatively, the number of polar residues, such as Q, could be systematically increased to determine whether a sufficient percentage of them would create a discernible effect. It is the flexibility of the guest residue sites in ELPs that makes them ideal substrates for such investigations.

(60) Luan, C. H.; Urry, D. W. *J. Phys. Chem.* **1991**, *95*, 7896–7900.

(61) Li, B.; Alonso, D. O. V.; Bennion, B. J.; Daggett, V. *J. Am. Chem. Soc.* **2001**, *123*, 11991–11998.

(62) Maeda, Y.; Nakamura, T.; Ikeda, I. *Macromolecules* **2001**, *34*, 8246–8251.

(63) The ELPs used here have a leader sequence of SKGPG and a trailer sequence of WP.

(59) Zhang, Y. J.; Trabbic-Carlson, K.; Albertorio, F.; Chilkoti, A.; Cremer, P. S. *Biomacromolecules* **2006**, *7*, 2192–2199.

Acknowledgment. This work was supported by the National Science Foundation (Grant CHE-0809854 to P.S.C.), the Robert A. Welch Foundation (Grants A-1421 to P.S.C. and BE-1281 to J.M.S.), and the National Institutes of Health (Grant RO1 GM61232 to A.C.). We also thank Dr. Katherine Cimatu for useful discussions.

Supporting Information Available: Additional CD data as a function of temperature and DSC data for the other four ELPs. This material is available free of charge via the Internet at <http://pubs.acs.org>.

JA9040785